



CHORUS

This is the accepted manuscript made available via CHORUS. The article has been published as:

Probing the Higgs Couplings to Photons in $h \rightarrow 4\ell$ at the LHC

Yi Chen, Roni Harnik, and Roberto Vega-Morales

Phys. Rev. Lett. **113**, 191801 — Published 4 November 2014

DOI: [10.1103/PhysRevLett.113.191801](https://doi.org/10.1103/PhysRevLett.113.191801)

Probing the Higgs Couplings to Photons in $h \rightarrow 4\ell$ at the LHC

Yi Chen^a, Roni Harnik^b, Roberto Vega-Morales^c

^a*Lauritsen Laboratory for High Energy Physics, California Institute of Technology, Pasadena, CA, 92115,*

^b*Theoretical Physics Department, Fermilab, P.O. Box 500, Batavia, IL 60510, USA,*

^c*Laboratoire de Physique Théorique d'Orsay, UMR8627-CNRS, Université Paris-Sud, Orsay, France**

We explore the sensitivity of the Higgs decay to four leptons, the so-called golden channel, to higher dimensional loop-induced couplings of the Higgs boson to ZZ , $Z\gamma$, and $\gamma\gamma$ pairs, allowing for general CP mixtures. The larger standard model tree level coupling $hZ^\mu Z_\mu$ is the dominant “background” for the loop induced couplings. However this large background interferes with the smaller loop induced couplings, enhancing the sensitivity. We perform a maximum likelihood analysis based on analytic expressions of the fully differential decay width for $h \rightarrow 4\ell$ ($4\ell \equiv 2e2\mu, 4e, 4\mu$) including all interference effects. We find that the spectral shapes induced by Higgs couplings to photons are particularly different than the $hZ^\mu Z_\mu$ background leading to enhanced sensitivity to these couplings. We show that even if the $h \rightarrow \gamma\gamma$ and $h \rightarrow 4\ell$ rates agree with that predicted by the Standard Model, the golden channel has the potential to probe both the CP nature as well as the overall sign of the Higgs coupling to photons well before the end of a high-luminosity LHC.

INTRODUCTION

With the recent discovery of the Higgs boson at the LHC [1, 2] the focus now shifts to the determination of its detailed properties and in particular whether or not it possesses any anomalous couplings not predicted by the Standard Model (SM). The Higgs decay to electrons and muons through electroweak gauge bosons, the so called golden channel, has been well established as a means towards accomplishing this goal as evidenced by the many studies of this channel [3–30]. Various methods were established to probe the Higgs couplings to ZZ pairs motivating experimental studies of their CP properties [31–33] where CP odd/even mixtures as large as $\sim 40\%$ are found to still be allowed. However, apart from recent studies [34–37], the potential for the $h \rightarrow 4\ell$ ($4\ell \equiv 2e2\mu, 4e, 4\mu$) decay to probe the Higgs couplings to $Z\gamma$ and $\gamma\gamma$ pairs (we do not distinguish between on/off-shell vector bosons) has largely been neglected.

It is typically thought that these contributions are too small to be detected in the golden channel since they only first occur at loop level with the photon forced to be off-shell. The study of these couplings is thus done solely using the rates of the decays $h \rightarrow Z\gamma$ and $h \rightarrow \gamma\gamma$ respectively. In this note we show that large differences in shapes of the kinematic distributions allow for the possi-

bility of measuring these couplings in the golden channel even if no significant deviations from the SM prediction are seen in the overall decay rates of $h \rightarrow \gamma\gamma$, $h \rightarrow 4\ell$, or $h \rightarrow Z\gamma$. Interference effects, in particular those with the tree level SM $hZ^\mu Z_\mu$ operator, also allow for the CP properties of these couplings to be studied.

The sensitivity to the loop induced couplings of the Higgs to photons is especially strong. Using a maximum likelihood analysis based on an analytic framework developed in [36], we find that the golden channel has excellent prospects to begin directly probing these couplings during LHC running with $\sim 100 - 400 fb^{-1}$ of luminosity (depending on detector performance and production uncertainties) with less optimistic prospects for the $Z\gamma$ and even less so for the loop induced ZZ couplings

EXAMINING THE GOLDEN CHANNEL

Higgs Couplings to EW Bosons

We consider the leading contributions to the Higgs couplings to neutral electroweak gauge bosons allowing for general CP odd/even mixtures as well as for ZZ , $Z\gamma$ and $\gamma\gamma$ to contribute simultaneously. These couplings are parametrized by the following Lagrangian,

$$\begin{aligned} \mathcal{L} \supset \frac{h}{4v} & \left(2A_1^{ZZ} m_Z^2 Z^\mu Z_\mu + A_2^{ZZ} Z^{\mu\nu} Z_{\mu\nu} + A_3^{ZZ} Z^{\mu\nu} \tilde{Z}_{\mu\nu} \right. \\ & \left. + 2A_2^{Z\gamma} F^{\mu\nu} Z_{\mu\nu} + 2A_3^{Z\gamma} F^{\mu\nu} \tilde{Z}_{\mu\nu} + A_2^{\gamma\gamma} F^{\mu\nu} F_{\mu\nu} + A_3^{\gamma\gamma} F^{\mu\nu} \tilde{F}_{\mu\nu} \right), \end{aligned} \quad (1)$$

where we have taken h real. We consider only up to dimension five operators and Z_μ is the Z field while $V_{\mu\nu} = \partial_\mu V_\nu - \partial_\nu V_\mu$ are the usual bosonic field strengths. The

dual field strengths are defined as $\tilde{V}_{\mu\nu} = \frac{1}{2} \epsilon_{\mu\nu\rho\sigma} V^{\rho\sigma}$. We work within Higgs effective theory and approximate all couplings to be real, dimensionless, and constant.

The Fully Differential Decay Rate

For the purpose of our analysis it is useful to note that the fully differential decay width for $h \rightarrow 4\ell$ [35, 36] is a sum over terms quadratic in the couplings which we can write schematically as,

$$\frac{d\Gamma_{h \rightarrow 4\ell}}{d\mathcal{O}} \sim \sum A_n^i A_m^{j*} \times \frac{d\hat{\Gamma}_{nm}^{ij}}{d\mathcal{O}}, \quad (2)$$

where the sum is over $n, m = 1, 2, 3$ and $i, j = ZZ, Z\gamma, \gamma\gamma$ (note $A_1^{Z\gamma} = A_1^{\gamma\gamma} = 0$). We also define $d\mathcal{O} = dM_1^2 dM_2^2 d\vec{\Omega}$ which represents the differential volume element, or phase space, in terms of two invariant masses corresponding to the two lepton pairs (M_1, M_2) and five angles ($\vec{\Omega}$) [36, 37]. It will also be useful to define,

$$\frac{d\Gamma_{nm}^{ij}}{d\mathcal{O}} \equiv A_n^i A_m^{j*} \times \frac{d\hat{\Gamma}_{nm}^{ij}}{d\mathcal{O}}. \quad (3)$$

The various projections for each combination of operators can be obtained from Eq.(3) by integration over the appropriate set of variables.

The Differential Mass Spectra

The power of the golden channel comes from the large number of observables available in the 4ℓ final state and their correlations which provide a vast amount of information. Focusing on only decay observables and taking the Higgs mass as input, we have the two invariant masses, corresponding to the two lepton pairs, and three angles of relevance as discussed above (see [35–37] for more details). The shapes of the distributions, $d\Gamma_{nm}^{ij}/d\mathcal{O}$ in Eq.(3), are in general quite different for the various $ZZ, Z\gamma$ and $\gamma\gamma$ contributions allowing for strong discriminating power between the different possible operators.

Since the invariant masses serve as such strongly discriminating variables [18, 38–40], we examine these distributions to get a qualitative picture of the relative sensitivity. These are presented in Fig. 1 for the $2e2\mu$ final state where we show the distributions for the invariant mass which reconstructs closest to the Z mass which we call M_1 and the ‘off-shell’ invariant mass which we call M_2 . We show the distributions (all normalized to one) for the four CP even operators squared corresponding to $|A_1^{ZZ}|^2$, $|A_2^{ZZ}|^2$, $|A_2^{Z\gamma}|^2$, and $|A_2^{\gamma\gamma}|^2$. One can see that for both the M_1 and M_2 distributions, the shape of $|A_2^{\gamma\gamma}|^2$ (green) is the operator most easily distinguished from the $|A_1^{ZZ}|^2$ ‘background’ (black). The next most distinguishable operator, mostly in M_2 , is $|A_2^{Z\gamma}|^2$ (orange) followed by $|A_2^{ZZ}|^2$ (blue) which as expected most closely resembles the $|A_1^{ZZ}|^2$ background. Shapes for CP odd squared terms follow a similar pattern and are thus not shown.

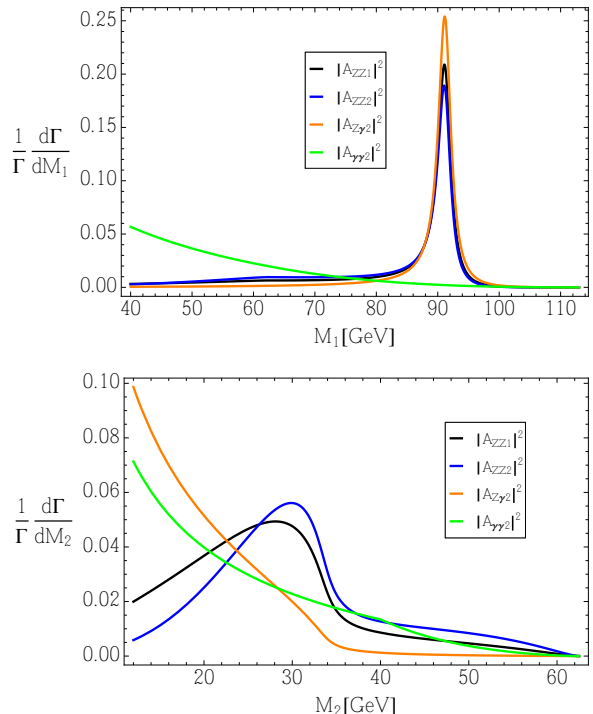


FIG. 1. **Top:** The normalized differential mass spectrum for M_1 in the $2e2\mu$ final state for the CP even terms squared plotted on top of the SM ‘background’ shown in black. **Bottom:** The differential mass spectrum for M_2 in the $2e2\mu$ final state for the same combination of operators.

The Integrated Magnitudes

It is also illuminating to show what we call the *integrated magnitude* of the various combination of operators defined for each pair of couplings as,

$$\Pi_{nm}^{ij} = A_n^i A_m^{j*} \times \int \left| \frac{d\hat{\Gamma}_{nm}^{ij}}{d\mathcal{O}} \right| d\mathcal{O}, \quad (4)$$

where the Π_{nm}^{ij} are strictly non-zero even in the case of CP violation. We show in Fig. 2 all possible combinations of Π_{nm}^{ij} for $A_1^{ZZ} = 2$, corresponding to the *tree level* SM value, while all loop induced couplings are set to one. We then normalize to the (tree level) SM value for the $h \rightarrow 4\ell$ decay width ($\Gamma_{4\ell}^{SM}$). The values shown are for $\Pi_{nm}^{ij}/\Gamma_{4\ell}^{SM}$ in the $2e2\mu$ final state [36] with cuts and reconstruction corresponding to a ‘CMS-like’ phase space [2] (defined in the results section). By examining the diagonal terms we see that the largest integrated magnitudes are for the $Z\gamma$ and $\gamma\gamma$ contributions while the tree level SM contribution given by the diagonal A_1^{ZZ} entry is equal to one by definition.

The values in Fig. 2 were obtained for all loop induced couplings set equal to one. Of course in the SM and in most new physics models we expect these couplings to be $\lesssim \mathcal{O}(10^{-2} - 10^{-3})$ or much smaller. We therefore again

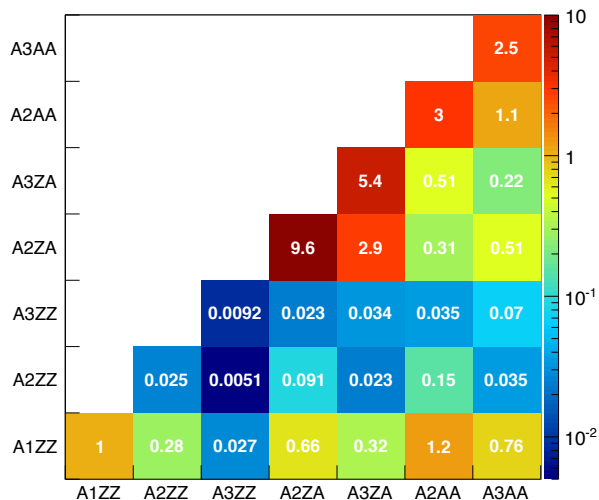


FIG. 2. The total integrated magnitudes, Π_{nm}^{ij} , defined in Eq.(4), which correspond to the pairs of couplings $A_n^i A_m^{j*}$. To obtain the values here we have set $A_1^{ZZ} = 2$ with all other couplings to one and normalized to the (tree level) SM value for the $h \rightarrow 4\ell$ decay width (see text).

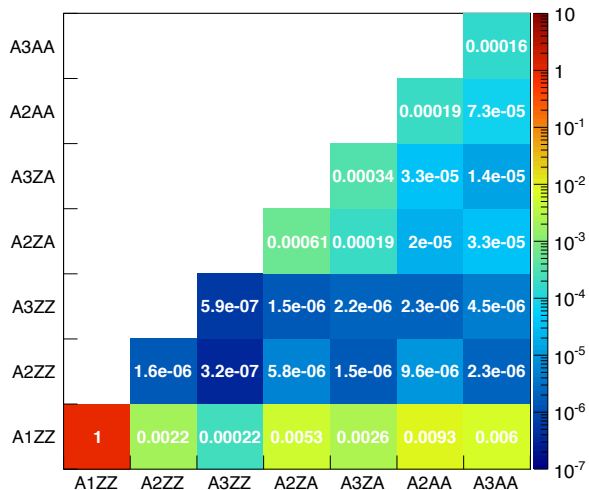


FIG. 3. The same as Fig. 2, but with $A_1^{ZZ} = 2$ and all other couplings to ~ 0.008 .

show $\Pi_{nm}^{ij}/\Gamma_{4\ell}^{SM}$ for the $2e2\mu$ final state in Fig. 3, but now with $A_1^{ZZ} = 2$ and all loop induced couplings set to ~ 0.008 . The SM combination $|A_1^{ZZ}|^2$ is equal to one (by definition). Of the others, the interference terms between the signal operators and A_1^{ZZ} dominate.

From these discussions we expect that we should have the strongest sensitivity to the $\gamma\gamma$ couplings followed by the $Z\gamma$ couplings and the weakest sensitivity to the loop induced ZZ couplings. As we will show below, this indeed turns out to be the case.

RESULTS

To obtain our results we use the framework developed and described in detail in [36]. We will take the SM *tree level* prediction of $A_1^{ZZ} = 2$ as input and fit to the remaining six couplings *simultaneously*. For all of our results we combine the $2e2\mu$, $4e$, and 4μ channels by computing the fully differential decay width for each final state [35, 36] (including identical final state interference for $4e$ and 4μ) and combining them into one likelihood.

Fit and Phase Space Definition

We define our six dimensional parameter space as,

$$\vec{A} = (A_2^{ZZ}, A_3^{ZZ}, A_2^{Z\gamma}, A_3^{Z\gamma}, A_2^{\gamma\gamma}, A_3^{\gamma\gamma}). \quad (5)$$

To estimate the sensitivity we obtain what we call an ‘effective’ σ or *average error* defined as [41],

$$\sigma = \sqrt{\frac{\pi}{2}} \langle |\hat{A} - \vec{A}_o| \rangle, \quad (6)$$

where \hat{A} is the value of the best fit parameter point obtained by maximization of the likelihood with respect to \vec{A} . Here \vec{A}_o represents the ‘true’ value with which our data sets are generated. We then find σ by conducting a large number of pseudoexperiments with a fixed number of events and obtaining a distribution for \hat{A} which will have some spread centered around the average value. We then translate the width of this distribution into our effective σ which converges to the usual interpretation of σ when the distribution for \hat{A} is perfectly gaussian.

We take the Higgs mass to be $m_h = 125$ GeV and limit our phase space to approximate that used by CMS as indicated by the following cuts and reconstruction:

- $p_{T\ell} > 20, 10, 7, 7$ GeV for lepton p_T ordering,
- $|\eta_\ell| < 2.4$ for the lepton rapidity,
- $40 \text{ GeV} \leq M_1$ and $12 \text{ GeV} \leq M_2$.

Here M_1 and M_2 are the reconstructed masses of the two lepton pairs. In reconstructing M_1 and M_2 we always impose $M_1 > M_2$ and take M_1 to be the reconstructed invariant mass for a particle and anti-particle pair which is closer to the Z mass.

Sensitivity as Function of Number of Events

Using the definition in Eq.(5) we fit to a ‘true’ parameter point $\vec{A}_o = (0, 0, 0, 0, 0, 0)$ which corresponds to the tree level SM prediction and holds at loop level until getting to a precision of $\mathcal{O}(10^{-2} - 10^{-3})$. In Fig. 4 we show the result for σ vs N_S for the six parameters defined in

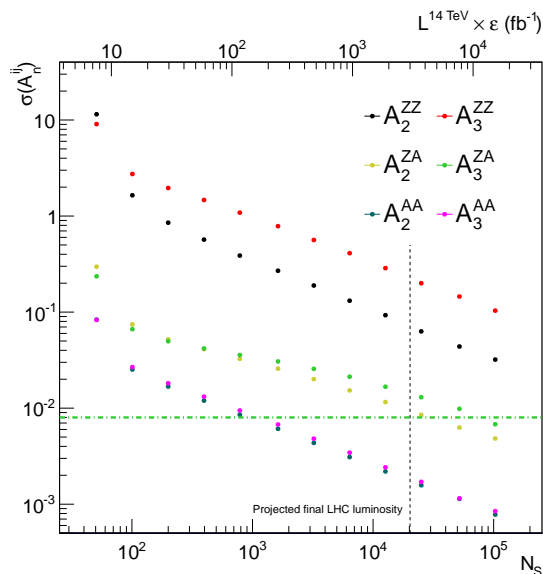


FIG. 4. The results for the effective σ defined in Eq.(6) of each coupling as a function of the number of signal events N_S for a true point $\vec{A}_o = (0, 0, 0, 0, 0, 0)$ (see text). Error bars are shown, but they are smaller than the dot sizes.

Eq.(1). We indicate by the green dashed line the value ~ 0.008 , corresponding to the magnitude of the leading order SM prediction for $A_2^{\gamma\gamma}$ at 125 GeV [42]. On the top axis we also show an estimate for the expected LHC luminosity multiplied by efficiency while the vertical gray dashed line indicates a rough estimate for the final LHC luminosity which will be achieved ($\sim 3000 fb^{-1}$). We have used production cross sections for both gluon fusion and vector boson fusion as well as the $h \rightarrow 4\ell$ branching fraction values provided by the LHC Higgs Cross Section Working Group [43, 44].

We see in Fig. 4 that the sensitivity to the $\gamma\gamma$ couplings is significantly greater than for $Z\gamma$ and even more so than for ZZ . This was to be expected from our considerations of the differential spectra as well as integrated magnitudes defined in Eq.(4). In fact we see that for the $\gamma\gamma$ couplings, $\sigma(A_{2,3}^{\gamma\gamma})$ reaches values $\lesssim \mathcal{O}(10^{-2})$ with $\gtrsim 800$ events which corresponds to roughly $100 fb^{-1}$ of luminosity assuming 100% efficiency. We estimate this number of events can be reached with $\sim 300 - 400 fb^{-1}$ after accounting for detector efficiencies [32].

Establishing the $h\gamma\gamma$ CP Properties

The results shown in Fig. 4 indicate that the golden channel should be able to establish the CP nature and overall sign of the Higgs couplings to photons for couplings roughly of the same size as those predicted by the SM. To demonstrate this we perform a second parameter extraction. This time we fit to the ‘true’ point $\vec{A}_o = (0, 0, 0, 0, -0.008, 0)$ again allowing all couplings to

float. We have chosen $A_2^{\gamma\gamma} = -0.008$ which is the leading contribution predicted by the SM at 125 GeV [42].

We show in Fig. 5 the results for a large set of pseudoexperiments each containing 12800 events. This corresponds roughly to an integrated luminosity of $3000 fb^{-1}$ assuming a uniform efficiency of 60% [32]. We show fit results in the 2D plane for $A_2^{\gamma\gamma}$ vs $A_3^{\gamma\gamma}$ where the turquoise circles correspond to the 68% and 95% confidence intervals obtained in our fit. The pink ring indicates the projected 1σ confidence interval which will be achieved in the $h \rightarrow \gamma\gamma$ decay channel [45] for the same luminosity. The pink ring makes it clear that the $h \rightarrow \gamma\gamma$ process is only sensitive to the combination $|A_2^{\gamma\gamma}|^2 + |A_3^{\gamma\gamma}|^2$ and thus can not directly probe the CP nature of these couplings. We also show in the thin green line the very strong, but highly model dependent, constraint coming from the electron EDM [46, 47]. For this constraint we have assumed the couplings of the Higgs to first generation fermions is of order their SM value and that the mass of the states which generate these operators is $\sim \text{TeV}$. This constraint can be completely relaxed in other models [46]. The green line makes it clear that even with these model dependent assumptions, EDM measurements can not establish the overall sign of the Higgs photon coupling.

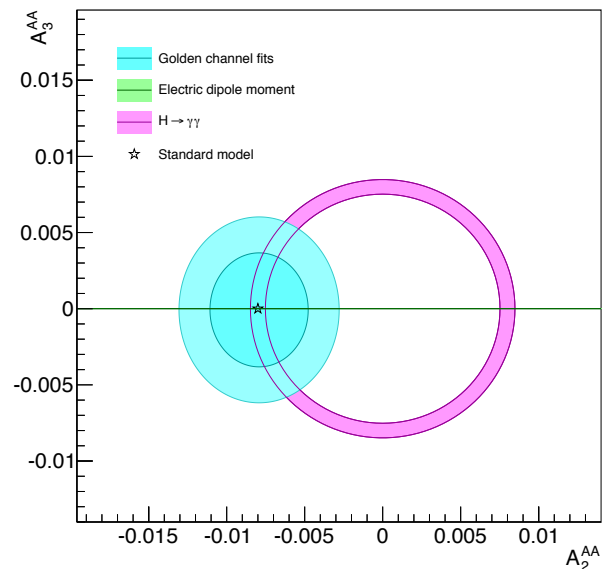


FIG. 5. The results of our parameter extraction (turquoise circles) in $h \rightarrow 4\ell$ for the true point $\vec{A}_o = (0, 0, 0, 0, -0.008, 0)$ (represented by the star) compared to $h \rightarrow \gamma\gamma$ rate (pink ring) and EDM constraints (thin green line).

CONCLUSIONS

We have examined the expected sensitivity of the $h \rightarrow 4\ell$ golden channel to the loop induced couplings of the Higgs boson to ZZ , $Z\gamma$, and $\gamma\gamma$ gauge boson pairs for values approximating those predicted by the Stan-

dard Model. We have demonstrated qualitatively that the golden channel has excellent prospects of directly establishing the CP nature of the Higgs couplings to photons, well before the end of LHC running, with less optimistic prospects for the ZZ and $Z\gamma$ loop induced couplings.

Specifically, we find that for standard ‘CMS-like’ cuts and reconstruction with $\sim 100 - 400 fb^{-1}$ of luminosity the LHC will reach the precision necessary to begin distinguishing between zero and values corresponding to the loop induced Standard Model effects which generate the Higgs coupling to photons and, in particular, the overall sign of this coupling can be established. This of course warrants further study, but indicates that the golden channel is capable of directly probing the CP properties of the Higgs couplings to photons at the LHC, something which is not currently possible by any other means.

Acknowledgments: R.V.M. is supported by the ERC Advanced Grant Higg@LHC. Fermilab is operated by Fermi Research Alliance, LLC, under Contract No. DE-AC02-07CH11359 with the United States Department of Energy. Y.C. is supported by the Weston Havens Foundation and DOE grant No. DE-FG02-92-ER-40701. This work is also sponsored in part by the DOE grant No. DE-FG02-91ER40684. This work used the Extreme Science and Engineering Discovery Environment (XSEDE), which is supported by National Science Foundation grant number OCI-1053575.

* yichen@caltech.edu
roni@fnal.gov
roberto.vega@th.u-psud.fr

- [1] G. Aad et al. (ATLAS Collaboration), *Phys.Lett.* **B716**, 1 (2012), 1207.7214.
- [2] S. Chatrchyan et al. (CMS Collaboration), *Phys.Lett.* **B716**, 30 (2012), 1207.7235.
- [3] C. A. Nelson, *Phys.Rev.* **D37**, 1220 (1988).
- [4] A. Soni and R. Xu, *Phys.Rev.* **D48**, 5259 (1993), hep-ph/9301225.
- [5] D. Chang, W.-Y. Keung, and I. Phillips, *Phys.Rev.* **D48**, 3225 (1993), hep-ph/9303226.
- [6] V. D. Barger, K.-m. Cheung, A. Djouadi, B. A. Kniehl, and P. Zerwas, *Phys.Rev.* **D49**, 79 (1994), hep-ph/9306270.
- [7] T. Arens and L. Sehgal, *Z.Phys.* **C66**, 89 (1995), hep-ph/9409396.
- [8] S. Choi, . Miller, D.J., M. Muhlleitner, and P. Zerwas, *Phys.Lett.* **B553**, 61 (2003), hep-ph/0210077.
- [9] C. Buszello, I. Fleck, P. Marquard, and J. van der Bij, *Eur.Phys.J.* **C32**, 209 (2004), hep-ph/0212396.
- [10] R. M. Godbole, . Miller, D.J., and M. M. Muhlleitner, *JHEP* **0712**, 031 (2007), 0708.0458.
- [11] V. Kovalchuk, *J.Exp.Theor.Phys.* **107**, 774 (2008).
- [12] Q.-H. Cao, C. Jackson, W.-Y. Keung, I. Low, and J. Shu, *Phys.Rev.* **D81**, 015010 (2010), 0911.3398.
- [13] Y. Gao, A. V. Gritsan, Z. Guo, K. Melnikov, M. Schulze, et al., *Phys.Rev.* **D81**, 075022 (2010), 1001.3396.
- [14] A. De Rujula, J. Lykken, M. Pierini, C. Rogan, and M. Spiropulu, *Phys.Rev.* **D82**, 013003 (2010), 1001.5300.
- [15] J. S. Gainer, K. Kumar, I. Low, and R. Vega-Morales, *JHEP* **1111**, 027 (2011), 1108.2274.
- [16] B. Coleppa, K. Kumar, and H. E. Logan (2012), 1208.2692.
- [17] S. Bolognesi, Y. Gao, A. V. Gritsan, K. Melnikov, M. Schulze, et al. (2012), 1208.4018.
- [18] R. Boughezal, T. J. LeCompte, and F. Petriello (2012), 1208.4311.
- [19] A. Belyaev, N. D. Christensen, and A. Pukhov (2012), 1207.6082.
- [20] P. Avery, D. Bourilkov, M. Chen, T. Cheng, A. Drozdetskiy, et al. (2012), 1210.0896.
- [21] J. M. Campbell, W. T. Giele, and C. Williams (2012), 1205.3434.
- [22] J. M. Campbell, W. T. Giele, and C. Williams (2012), 1204.4424.
- [23] B. Grinstein, C. W. Murphy, and D. Pirskhalava, *JHEP* **1310**, 077 (2013), 1305.6938.
- [24] T. Modak, D. Sahoo, R. Sinha, and H.-Y. Cheng (2013), 1301.5404.
- [25] Y. Sun, X.-F. Wang, and D.-N. Gao (2013), 1309.4171.
- [26] J. S. Gainer, J. Lykken, K. T. Matchev, S. Mrenna, and M. Park, *Phys.Rev.Lett.* **111**, 041801 (2013), 1304.4936.
- [27] M. Chen, T. Cheng, J. S. Gainer, A. Korytov, K. T. Matchev, et al. (2013), 1310.1397.
- [28] I. Anderson, S. Bolognesi, F. Caola, Y. Gao, A. V. Gritsan, et al. (2013), 1309.4819.
- [29] G. Buchalla, O. Cata, and G. D’Ambrosio (2013), 1310.2574.
- [30] J. S. Gainer, J. Lykken, K. T. Matchev, S. Mrenna, and M. Park (2014), 1403.4951.
- [31] S. Chatrchyan et al. (CMS Collaboration), *Phys.Rev.Lett.* **110**, 081803 (2013), 1212.6639.
- [32] S. Chatrchyan et al. (CMS Collaboration), *Phys.Rev.* **D89**, 092007 (2014), 1312.5353.
- [33] C. Collaboration (CMS Collaboration) (2014).
- [34] D. Stolarski and R. Vega-Morales (2012), 1208.4840.
- [35] Y. Chen, N. Tran, and R. Vega-Morales, *JHEP* **1301**, 182 (2013), 1211.1959.
- [36] Y. Chen and R. Vega-Morales (2013), 1310.2893.
- [37] Y. Chen, E. Di Marco, J. Lykken, M. Spiropulu, R. Vega-Morales, et al. (2014), 1401.2077.
- [38] G. Isidori, A. V. Manohar, and M. Trott, *Phys.Lett.* **B728**, 131 (2014), 1305.0663.
- [39] M. Gonzalez-Alonso and G. Isidori (2014), 1403.2648.
- [40] D. Curtin, R. Essig, S. Gori, P. Jaiswal, A. Katz, et al. (2013), 1312.4992.
- [41] Wikipedia (2013), http://en.wikipedia.org/wiki/Half-normal_distribution.
- [42] I. Low, J. Lykken, and G. Shaughnessy (2012), 1207.1093.
- [43] S. Dittmaier et al. (LHC Higgs Cross Section Working Group) (2011), 1101.0593.
- [44] S. Heinemeyer et al. (LHC Higgs Cross Section Working Group) (2013), 1307.1347.
- [45] W. Murray (2013), <http://indico.cern.ch/event/252045/session/3/contribution/8/material/slides/0.pdf>.
- [46] D. McKeen, M. Pospelov, and A. Ritz, *Phys.Rev.* **D86**, 113004 (2012), 1208.4597.
- [47] J. Baron et al. (ACME Collaboration), *Science* **343**, 269 (2014), 1310.7534.